Eur. J. Biochem. *148*, 119–126 (1985)

The binding of vanadium (V) oligoanions to sarcoplasmic reticulum

Sandor VARGA, Peter CSERMELY and Anthony MARTONOSI

Department of Biochemistry, State University of New York, Upstate Medical Center, Syracuse, New York

(Received September 14/December 7, 1984) – EJB 84 1002

The binding of monovanadate and decavanadate anions to sarcoplasmic reticulum vesicles was measured by equilibrium sedimentation. The affinity of vanadate binding and the molar amount of vanadium (V) bound at equilibrium is much greater with decavanadate than with monovanadate. The binding data can be rationalized in terms of one binding site per ATPase molecule for monovanadate and two sites per ATPase for decavanadate.

The Ca-ATPase crystals formed with monovanadate and with decavanadate are similar in appearance, but decavanadate is particularly effective in promoting the crystallization of Ca^{2+}-ATPase at low V concentration (10–100 μM) in a Ca^{2+}-free medium.

Two-dimensional arrays of Ca^{2+}-transport ATPase molecules develop in sarcoplasmic reticulum vesicles exposed to Na_3VO_4 in a Ca^{2+}-free medium [1–9]. Vanadate is assumed to bind with high affinity to the phosphate acceptor site of the Ca^{2+}-ATPase; as a result the E_2-vanadate complex accumulates with inhibition of ATPase activity and of the phosphorylation of the enzyme by inorganic orthophosphate [10, 11]. In agreement with this interpretation, interaction of Ca^{2+} with the high-affinity binding site of the Ca^{2+}-ATPase prevents the formation of Ca^{2+} ATPase crystals and disrupts the crystals that were formed previously in the absence of calcium [1, 3]. Inhibition of vanadate-induced crystallization was also observed in the presence of 5 mM Mg-ATP [1–3]. Ca^{2+} and ATP are expected to stabilize the E_1 conformation of the ATPase and therefore shift the equilibrium from the E_2 toward the E_1 form.

The rate of crystallization of Ca^{2+}-ATPase is markedly enhanced by increasing the vanadate concentration of the medium to 5 mM [1, 3]; this is surprising since essentially complete inhibition of ATPase activity was observed at less than 0.5 mM vanadate concentration. These observations suggested that inhibition of ATPase activity through the formation of a kinetically stable E_2-V enzyme complex may be a required but not sufficient condition for rapid crystallization to occur. There are at least two additional mechanisms that may be involved in the massive increase of the rate of crystallization of Ca^{2+}-ATPase at millimolar Na_3VO_4 concentration. (a) Vanadate may bind to low-affinity sites on the Ca^{2+}-ATPase, stabilizing the conformation that is most compatible with the formation of crystalline arrays. (b) The Ca^{2+}-ATPase may interact with one or more of the large number of oligomeric vanadate species that accumulate in aqueous solutions containing millimolar concentrations of vanadium (V) at neutral pH [12–14]. The tetrahedrally coordinated dimer ($V_2O_7^{5-}$), and tetramer ($V_4O_{12}^{4-}$) interconvert rapidly with monomeric vanadate [12], while the octahedrally coordinated decavanadate, $V_{10}O_{28}^{6-}$, is kinetically inert.

There is good evidence that phosphotransferases, such as phosphofructokinase [15], adenylate kinase [16–18], and hexokinase [12, 19], are inhibited only by the large octahedrally coordinated decameric vanadium (V) polyanion; in these systems the monomeric vanadate anion, or its lower tetrahedral polyanionic species are ineffective. In the case of phosphorylase all oligomeric forms are inhibitory, while monomeric vanadate activates the enzyme slightly [20]. Finally the K_i of 4 nM for the inhibition of Na, K-ATPase by vanadate [21] strongly argues for monomeric vanadate anion being the inhibitory species; there is no evidence implicating vanadium polymers in the inhibition.

In this report we correlate the binding of monovanadate and decavanadate to sarcoplasmic reticulum vesicles with their effects on the crystallization of the Ca^{2+}-ATPase and on the rate of Ca^{2+}-activated ATP hydrolysis. The results suggest that both monovanadate and decavanadate inhibit the Ca^{2+}-stimulated ATP hydrolysis, but decavanadate is particularly effective in promoting the crystallization of Ca^{2+}-ATPase. Therefore, in addition to the formation of the stable E_2-vanadate intermediate, coordination of the large octahedral decavanadate at or near the active site may be required to stabilize the ezyme conformation that is suitable for the crystallization of the Ca^{2+}-ATPase.

MATERIALS AND METHODS

Sarcoplasmic reticulum vesicles were prepared from predominantly white skeletal muscles of rabbits as described earlier [22].

Preparation of monovanadate and decavanadate solutions

Aequeous solutions of vanadium (V) form a complex system consisting of a dozen or more molecular species [12–14]; their proportions are dependent upon the pH, vanadium concentration, temperature, and the ionic composition of the

Correspondence to: A. Martonosi, Department of Biochemistry, State University of New York, Upstate Medical Center, 766 Irving Avenue, Syracuse, New York, USA 13210.

S. Varga is on leave from the Central Research Laboratory of the University Medical School of Debrecen, Hungary. P. Csermely is on leave from the 1st Institute of Biochemistry, Semmelweis University Medical School, Budapest, Hungary.

incubation medium. At pH 7.4 and at a total vanadium concentration of 10 μM, the $H_2VO_4^-$ anion is the dominant species in rapid equilibrium with a small amount of tetrahedrally coordinated vanadium oligomers. With increasing vanadium concentration the concentration of vanadate oligomers increases and, at millimolar concentration, oligomers become major components of the system.

In these experiments stock solutions of monovanadate were prepared by boiling freshly made aequeous solutions of Na_3VO_4 (Fisher Scientific Co.) at pH 10 for 15 min followed immediately by dilution to the final concentrations indicated in the figure legends.

Decavanadate solutions were prepared by adjusting the pH of a 50 mM Na_3VO_4 solution to 2.0; acid pH favors the accumulation of the orange-yellow decavanadate species. After 6–12 h the pH was adjusted to 7.4 at 2°C and the solution was used immediately for experiments. Under these conditions the decomposition of decavanadate is relatively slow, and even in dilute solutions, after 4 days of incubation at 2°C decavanadate remains a major species in solution. The rate of decomposition of decavanadate at neutral pH sharply increases with temperature. Therefore care must be taken to use only freshly prepared, ice-cold decavanadate stock solution.

Electron microscopy

The vesicle suspensions containing 0.1 M KCl, 10 mM imidazole, pH 7.4, 5 mM $MgCl_2$, 0.5 mM EGTA and 1 mg microsomal protein/ml were incubated with monovanadate or decavanadate at total concentrations ranging over 0–5 mM at 4°C for 4–96 h. For electron microscopy, the vesicle suspensions were placed on carbon-coated parlodion films and stained with freshly prepared 1% uranyl acetate (pH 4.3). The specimens were viewed with a Siemens Elmiskop I electron microscope at 60 kV accelerating voltage. For magnification calibration, catalase crystals negatively stained with 1% uranyl acetate were used [23]. The extent of crystallization of Ca^{2+}-ATPase, denoted as 'crystallization index', was determined by counting about 500–1000 vesicles in random fields of electron micrographs and expressing the number of vesicles with crystalline regions on their surface as a percentage of the total vesicle number. The electron micrographs were scored by four independent observers and the crystallization index represents the average of four counts that were usually in good agreement. The crystallization index proved to be a simple and reliable indicator of the extent of crystallization under various experimental conditions and in microsome preparations isolated from different muscle types of several animal species. Nevertheless it must be viewed as a semiquantitative measure of crystallization. Attempts at estimating the area of crystalline regions as a percentage of the total vesicle surface area did not give acceptable results for several technical reasons outlined earlier [9] and were not pursued further.

Measurement of vanadate binding to microsomes

The binding of vanadate was measured after incubation of microsomes (1–10 mg protein/ml) in a solution of 0.1 M KCl, 10 mM imidazole pH 7.4, 5 mM $MgCl_2$, 0.5 mM EGTA and monovandate or decavanadate at V concentrations ranging over 0–5 mM. The total volume of the assay mixture was 2 ml and all assays were performed in plastic containers to minimize interference by the vanadate content of glass. After incubation for 2–96 h at 4°C the microsomes were removed by centrifugation for 30 min at $100000 \times g$. The supernatant was collected for the determination of free vanadate concentration. Two methods were used for the measurement of vanadate binding.

In method 1 the amount of vanadate bound to the microsomes was determined from the difference between the vanadate concentrations of the supernatants obtained after removal of microsomes by centrifugation, and the vanadate concentration of microsome-free control samples subjected to centrifugation under identical conditions. There was no indication of vanadate binding to the centrifuge tubes or of significant sedimentation of vanadate under the conditions of these experiments. In method 2 the sedimented microsomes were washed twice with 5 ml ice-cold vanadate-free incubation medium and used for the determination of residual bound vanadate.

The concentration of monovanadate was measured by the method of Goodno [24, 25], using the metallochromic dye 4-(2-pyridylazo)-resorcinol as indicator. Decavanadate concentration was determined by two methods. In method A, the orange-yellow colour of decavanadate was measured at 400 nm in the supernatant obtained after sedimentation of the microsomes. The sedimented microsomes were also analyzed after solubilization in 4% sodium dodecylsulfate. In method B the decavanadate was converted into monovanadate by heating the solutions at 90°C for 30 min; the monovanadate concentration was determined according to Goodno [24]. Appropriate control samples used for calibration indicate that upon heating at 90°C for 30 min, more than 90% of the decavanadate was converted into monovanadate. All data are expressed in molar amounts of vanadium.

The Lowry method [26] was used for the determination of protein concentration.

The measurement of ATPase activity

For measurement of Mg^{2+},Ca^{2+}-activated ATPase activity, microsomes were preincubated at 2°C in a medium of 0.1 M KCl, 10 mM imidazole pH 7.4, 5 mM $MgCl_2$, 0.5 mM EGTA, 1 mg microsomal protein/ml and either monovanadate or decavanadate at total V concentrations ranging over 0–2.5 mM. A23187 (2 μM) was also present in some experiments. After preincubation for 2–24 h at 2°C, 0.2-ml aliquots of the above suspension were diluted tenfold with a solution of 0.1 M KCl, 10 mM imidazole pH 7.4, 5 mM $MgCl_2$, 0.5 mM EGTA, 0.5 mM $CaCl_2$, 5 mM ATP with or without 1 μM A23187 and incubated at 25°C for 6 min. The reaction was stopped with trichloroacetic acid and the liberated inorganic phosphate was determined according to Fiske and Subbarow [27]. In control experiments Ca^{2+} was omitted from the ATPase assay medium to determine the Ca^{2+}-insensitive basal ATPase activity. The Ca-sensitive component of ATP hydrolysis was obtained by deducting the basal ATPase from the total (Mg^{2+} + Ca^{2+})-activated ATPase activity.

RESULTS

The binding of monovanadate to sarcoplasmic reticulum vesicles

The binding of vanadate to sarcoplasmic reticulum vesicles was measured at protein concentrations of 2 mg/ml and 5 mg/ml by equilibrating the microsomes with test solutions of 0.1 M KCl, 10 mM imidazole pH 7.4, 5 mM $MgCl_2$ and

0.5 mM EGTA at total vanadate concentrations ranging from 2.5 μM to 5 mM. After 2 h at 2°C the microsomes were sedimented by centrifugation at 100000 × *g* for 30 min and the amount of vanadate bound to the microsomes was determined from the decrease in the vanadate concentration of the supernatant (Fig. 1). The relationship between free V concentration and vanadate binding is complex. Up to about 500 μM V, monovanadate is the dominant species; the maximum number of monovanadate binding sites corresponding to this range of the binding curve is about 8–10 nmol V/mg microsomal protein, representing about 1 mol vanadate bound/mol Ca^{2+}-transport ATPase. The apparent dissociation constant is of the order of 50 μM. The sharp increase in vanadate binding above 500 μM free vanadate concentration is due to the presence of vanadate oligomers (dimers and tetramers) that increase in amount as the vanadate concentration rises [12].

Much of the bound vanadate is displaced from the sedimented microsomes by brief washing at 2°C with vanadate-free incubation medium (Fig. 1).

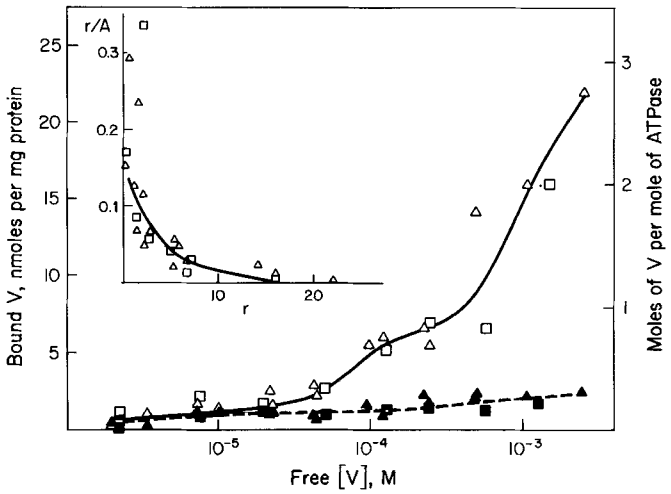

Fig. 1. *The binding of monovanadate to sarcoplasmic reticulum vesicles.* The sarcoplasmic reticulum vesicles were incubated in a standard medium consisting of 0.1 M KCl, 10 mM imidazole pH 7.4, 5 mM $MgCl_2$, 0.5 mM EGTA and total vanadate concentrations ranging from 2.5 μM to 5 mM, at 2°C for 2 h, followed by centrifugation at 100000 × *g* for 30 min. The free vanadate concentration in the supernatant was determined according to Goodno [24]. The open symbols represent the binding of vanadate determined from the supernatants by method 1, as described under Methods. The closed symbols are binding data obtained from the washed microsomal sediment according to method 2. The concentration of microsomal proteins was either 2 mg/ml (△, ▲) or 5 mg/ml (□, ■). The insert is a Scatchard plot of the data obtained by method 1. A is the free concentration of vanadate in μM; r denotes nmol vanadate bound/mg microsomal protein

The binding of decavanadate to sarcoplasmic reticulum vesicles

Stock solutions of Na_3VO_4 (50 mM) were adjusted to pH 2.0 for 2 h followed by neutralization and dilution to final concentrations ranging between 2.5 μM and 5 mM. The orange-yellow decavanadate species that forms at acidic pH is kinetically stable [12] and decomposes only rather slowly over a period of several days at 2°C (Fig. 2A). The rate of decavanadate hydrolysis was considerably faster ar 25°C (Fig. 2B). The decomposition in buffered solutions follows a pseudo-first-order kinetics. The kinetic constants calculated from the data of Fig. 2 are $k_{2°C} = 0.0084 \pm 0.0011\ h^{-1}$, $k_{25°C} = 0.165 \pm 0.01\ h^{-1}$. The activation energy is about 96 kJ/mol. These results are in the range of the previous literature data [28, 29]. The slow decomposition of decavanadate at 2°C permits the measurement of decavanadate binding even at relatively low free vanadate concentrations, where thermodynamically the vanadate monomer is the favored molecular species.

The binding of decavanadate to sarcoplasmic reticulum vesicles was determined as described under Methods, using the orange-yellow colour of decavanadate as a measure of its concentration (Fig. 3A). At protein concentrations of 1, 5, and 10 mg/ml the amount of decavanadate bound/mg microsomal protein reached maximum values of about 150 nmol V/mg protein (Fig. 3), that is 10–18 times greater than the maximum binding of monovanadate (Fig. 1). The binding shows positive cooperativity. Half-maximum saturation was at 50–100 μM V concentration, corresponding to a decavanadate concentration of 5–10 μM. The amount of bound decavanadate determined in the washed microsomal sediment was about two-thirds of the values obtained from assays in the supernatant. Under otherwise identical conditions the presence of 50 μM A23187 (at a protein concentration of 10 mg/ml) did not affect the binding of decavanadate. Essentially similar data were obtained using the 4-(2-pyridylazo)-resorcinol method for the assay of vanadate concentration after conversion of decavanadate into monovanadate by heating (Fig. 3B). Increasing the time of incubation from 2 h to 96 h did not alter significantly the decavanadate binding determined either by absorbance measurements at 400 nm, or after hydrolysis into monovanadate by the 4-(2-pyridylazo)-resorcinol method (not shown).

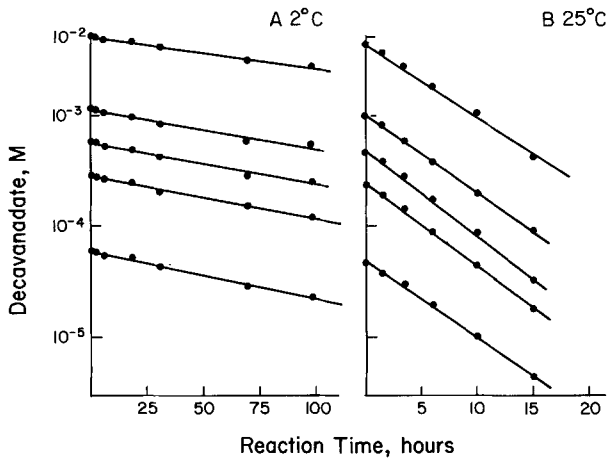

Fig. 2. *The decomposition of the decavanadate at pH 7.4 at different temperatures and total vanadate concentrations.* Samples contained 0.1 M KCl, 10 mM imidazole, pH 7.4, 5 mM $MgCl_2$, 0.5 mM EGTA and vanadate at five different total V concentrations. The decavanadate stock solutions (50 mM) were diluted to the final concentrations at the start of the experiment. The concentrations of decavanadate were determined by absorbance measurements at 400 nm. In (A) the incubation was carried out at 2°C, while in (B) the data show the decavanadate decay at 25°C

The effect of monovanadate and decavanadate on the crystallization of the Ca^{2+}-ATPase in sarcoplasmic reticulum

The rate of crystallization of Ca^{2+}-ATPase was measured at 2°C, at total vanadate concentrations ranging between

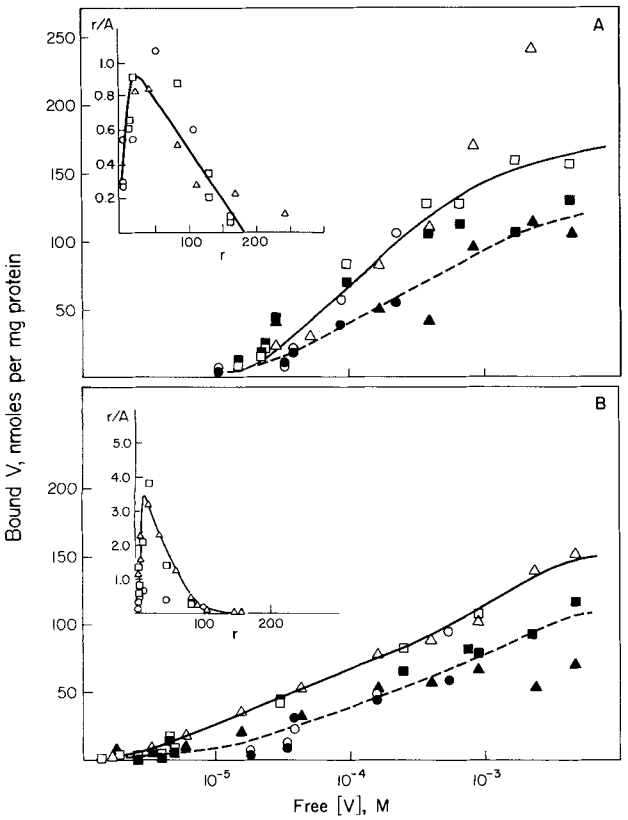

Fig. 3. *Decavanadate binding to sarcoplasmic reticulum vesicles at different protein concentrations.* (A) The vesicles were incubated in standard media in the cold room for 2 h at total vanadate concentrations ranging from 2.5 μM to 5 mM (expressed as monovanadate). The concentration of decavanadate was determined by absorbance measurements at 400 nm. The open symbols represent values determined by method 1 from the supernatants; the closed symbols are values calculated from the sediments according to method 2. Symbols: (△, ▲) vanadate binding at 1 mg/ml protein concentration; (□, ■) vanadate binding at 5 mg/ml protein concentration; (○, ●) vanadate binding at 10 mg/ml protein concentration, in the presence of 50 μM A23187. (B) The experiments were performed as described under A except that the concentration of decavanadate in the supernatant and in the sedimented microsomes was determined after conversion into monovanadate according to the method of Goodno [24]. Inserts are Scatchard plots of the same data where A is the free V concentration and r is nmol V bound/mg protein

50 μM and 5 mM over a 4-day period (Fig. 4). The extent of crystallization, defined as the crystallization index, is the number of vesicles with crystalline regions on their surface expressed as a percentage of the total number of about 500–1000 vesicles counted in random fields of electron micrographs. Under optimum conditions, in standard preparations of sarcoplasmic reticulum prepared from predominantly white skeletal muscles of rabbits, the crystallization index reaches 80–90%, i.e. 80–90% of the vesicles contain well-defined crystalline regions on at least portions of their surface. The crystallization indices were measured after 4 h, 24 h and 96 h of incubation at 2 °C with either decavanadate (Fig. 4A, C), or monovanadate (Fig. 4B, D), under conditions similar to those used in measurements of the vanadate binding (Fig. 3).

The relationships between the crystallization index and the total (Fig. 4B) or free (Fig. 4D) monovanadate concentrations are consistent with the binding data shown in Fig. 1. The similarity of the curves in Figs 4B and 4D is due to the fact that under the conditions of these experiments, at a protein concentration of 1 mg/ml, the binding of monovanadate to the microsomes has only slight effect on the free vanadate concentration. The concentration of monovanadate required to produce 50% crystallization decreased from ≈ 800 μM at 4 h to ≈ 500 μM at 24 h and ≈ 400 μM after 4 days. Above 1 mM vanadate concentration, vanadate polymers (dimers and tetramers) accumulate and they are likely to influence the crystallization process.

The striking effectiveness of decavanadate to promote crystallization of the Ca^{2+}-ATPase is illustrated in Fig. 4C. 50% crystallization is obtained at 150 μM V after 4 h, at 44 μM V after 24 h, and at 15 μM V after 4 days. These values correspond to 15 μM, 4.4 μM and 1.5 μM decavanadate respectively. The relationship between free decavanadate concentration and the extent of crystallization shows positive cooperatively (Fig. 4C). The cooperative character of the relationship between total decavanadate concentration and the crystallization index (Fig. 4A) in part arises from the massive binding of decavanadate to microsomes that causes a large decrease in free vanadate concentration even at protein concentrations as low as 1 mg/ml. As a result, below 0.1 mM total vanadate concentration, the limited availability of vanadate steepens the curve and enhances its cooperative character.

A23187 (5 μM) inhibited the crystallization of Ca^{2+}-ATPase induced by monovanadate but had little effect on the crystal formation in the presence of decavanadate (Fig. 5). These observations are consistent with the powerful stabilizing influence of decavanadate upon the two-dimensional crystals of Ca^{2+}-ATPase.

Inhibition of Ca^{2+}-modulated ATPase activity by monovanadate and decavanadate

The inhibition of Ca^{2+}-modulated ATPase activity by monovanadate and decavanadate was measured after preincubation of the vesicles with EGTA and vanadate under conditions similar to those used in the crystallization and vanadate binding studies (Fig. 6). In native sarcoplasmic reticulum vesicles preincubated with 0.5 mM EGTA for short periods of up to 2 h, the Ca^{2+}-modulated ATPase activity measured at steady state is slow because the Ca^{2+} accumulated within the vesicles inhibits the ATPase activity (Fig. 6A, C). Under these conditions the steady-state ATP hydrolysis corrected for basal ATPase activity is relatively insensitive to either monovanadate (Fig. 6A) or decavanadate (Fig. 6C). Preincubation with EGTA for 24 h at 2 °C increases the permeability of the vesicles for Ca^{2+} and increases the steady-state rate of ATP hydrolysis [30]. Under these conditions both monovanadate (Fig. 6A) and decavanadate (Fig. 6C), inhibit the steady-state rate of Ca^{2+}-modulated ATPase activity with an apparent K_i in the vicinity of ≈ 50 μM.

In the presence of 2 μM A23187, a Ca^{2+} ionophore, there is no net Ca^{2+} uptake due to the elimination of Ca^{2+} barriers, and the ATP hydrolysis continues in steady state at a rate near the initial velocity (Fig. 6B and D), irrespective of the duration of preincubation with EGTA. The inhibition of ATPase activity by monovanadate and decavanadate is strikingly evident under these conditions. The apparent K_i is about 50 μM total V concentration in both cases (Fig. 6B, D). The corresponding decavanadate concentration (Fig. 6D) would be about 5 μM. The K_i for inhibition of ATPase activity by

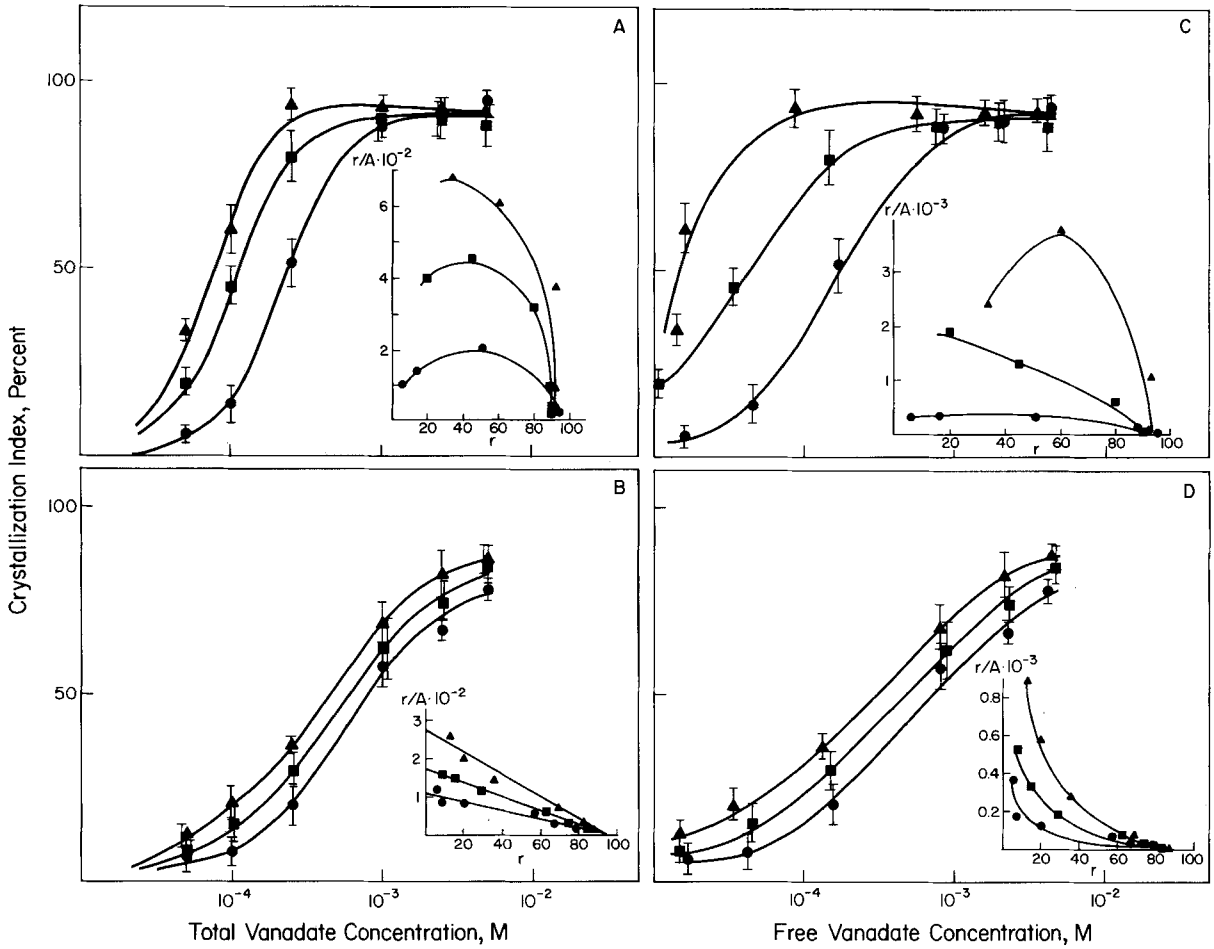

Fig. 4. *The relationship between the concentration of monovanadate and decavanadate and the rate of crystallization of Ca^{2+}-ATPase in sarcoplasmic reticulum.* Sarcoplasmic reticulum vesicles were incubated at 4°C in 0.1 M KCl, 10 mM imidazole, pH 7.4, 5 mM $MgCl_2$, 0.5 mM EGTA and Na_3VO_4 at the concentrations indicated. Samples were taken after 4 h (●——●), 24 h (■——■) and 4 days (▲——▲) for electron microscopy and negatively stained with 1% uranyl acetate, pH 4.3. The crystallization index denotes the number of vesicles with crystalline regions on their surface expressed as a percentage of the total number of vesicles. On average, 630 vesicles were counted for each data point and the standard error denotes the range of variation of the counts made by four independent observers. The crystallization indices obtained with decavanadate (A) or monovanadate (B) are plotted against the total molar vanadate concentration. The data of A and B were replotted in C and D, respectively, against the free vanadate concentration measured in a separate set of experiments, under conditions similar to those used in the electron microscope studies. The concentrations of decavanadate (A and C) and monovanadate (B and D) are all expressed as molar monovanadate to facilitate comparison. Inserts are the Scatchard plots of the same data sets; A is the total or free vanadate concentration, and r is the crystallization index

monovanadate and decavanadate is close to the concentrations of monovanadate and decavanadate that are required for half-maximal occupancy of vanadate binding sites and for half-maximal crystallization of the Ca^{2+}-ATPase. Therefore there is reasonable basis to assume that trapping of the enzyme in the E_2-V configuration and the related local coordination effects are responsible for the inhibition of Ca^{2+}-stimulated ATPase and for the crystallization of the Ca^{2+}-transport ATPase.

The rate of crystallization of Ca^{2+}-ATPase induced by decavanadate is not affected significantly by 5 μM A23187; at this relatively high concentration A23187 actually inhibits the crystallization of Ca^{2+}-ATPase induced by monovanadate. This is surprising since A23187 is apparently required for effective inhibition of ATPase activity by either monovanadate or decavanadate. This difference is presumably related to the fact that the assay of Ca^{2+}-modulated ATPase activity requires about 0.01 mM Ca^{2+} and 5 mM ATP, two agents that are absent from the crystallization system because they tend to disrupt Ca^{2+}-ATPase crystals. For this reason the physical state of the Ca^{2+}-ATPase in the ATPase activity measurements and in the crystallization assays is likely to be somewhat different.

As shown in Fig. 7, the rate of Ca^{2+}-modulated ATP hydrolysis after a 24-h incubation with vanadate and EGTA is still significant in the absence of A23187, although under similar conditions but without Ca^{2+} and ATP, the crystallization index is 80–90%. Only with A23187 did we achieve complete inhibition of ATP hydrolysis. These observations imply that addition of Ca^{2+} and ATP to the samples preincubated without A23187 causes partial reversal of the vanadate inhibition of ATPase activity; this effect is not observed in the presence of A23187.

DISCUSSION

In sarcoplasmic reticulum vesicles the maximum number of binding sites for monovanadate is 8–10 nmol V/mg pro-

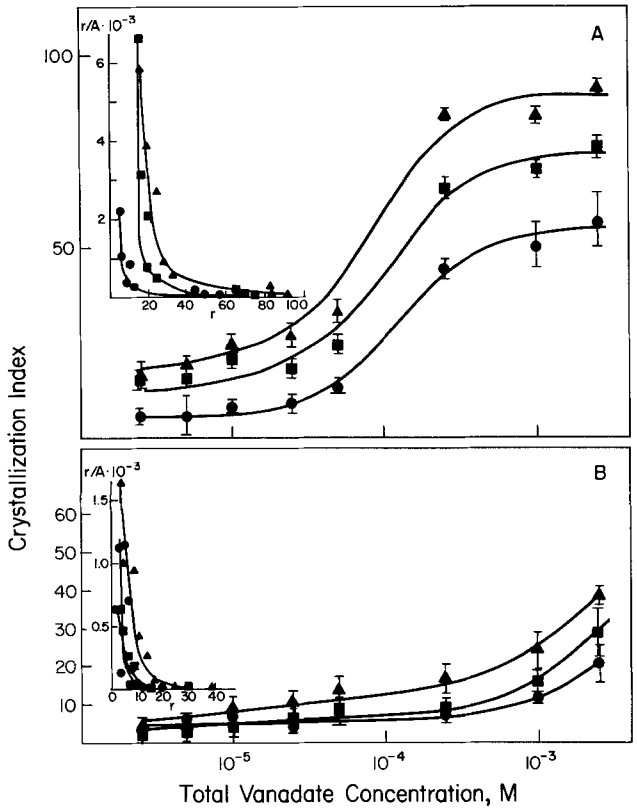

Fig. 5. *Effect of A23187 on crystallization of Ca^{2+}-ATPase in sarcoplasmic reticulum.* Sarcoplasmic reticulum vesicles were incubated at 4°C in 0.1 M KCl, 10 mM imidazole, pH 7.4, 5 mM $MgCl_2$, 0.5 mM EGTA and Na_3VO_4 at the concentrations indicated, in the presence of 5 μM A23187. Samples were taken after 4 h (●), 24 h (■) and 4 days (▲) for electron microscopy and negatively stained with 1% uranyl acetate, pH 4.3. The crystallization index denotes the number of vesicles with crystalline regions on their surface, expressed as a percentage of the total number of vesicles. On the average 400 vesicles were counted for each data point and the standard error denotes the range of variation of the counts made by four independent observers.Crystallization indices obtained with decavanadate (A) or monovanadate (B) are plotted against the total molar vanadate concentration. The insert is a Scatchard plot of the data. A is the free concentration of vanadate (μM); r denotes the crystallization index

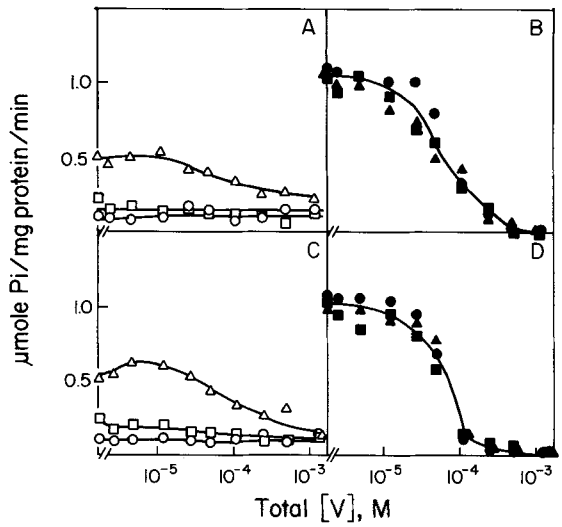

Fig. 6. *The effect of monovanadate and decavanadate on the hydrolysis of ATP by sarcoplasmic reticulum vesicles.* Sarcoplasmic reticulum vesicles were preincubated at 2°C with 0.1 M KCl, 10 mM imidazole, 5 mM $MgCl_2$, 0.5 mM EGTA for 0 (○, ●), 2 h (□, ■), or 24 h (△, ▲) with 2 μM A23187 (B and D) or without A23187 (A and C). After the preincubation, monovanadate (A and B) or decavanadate (C and D) were added to final total concentrations as indicated in the abscissa and the incubation continued for 2 h. All vanadate concentrations are expressed as molar monovanadate (V). At the end of incubation, aliquots were taken for the assay of ATP hydrolysis as described under Methods. The Ca^{2+}-activated component of ATP hydrolysis was calculated from the total ATPase activity after correction for the basal Mg-ATPase determined in the absence of Ca^{2+}. The basal ATPase is insensitive to vanadate

tein, corresponding to about 1 mol V bound/mol ATPase. The apparent dissociation constant is ≈ 50 μM. These values are in agreement with the observations of Medda and Hasselbach [25] and satisfactorily account for the inhibition of Ca^{2+}-modulated ATPase activity by monovanadate. It is plausible to assume that the binding site for monovanadate is in the vicinity of the phosphate-acceptor aspartyl group, and that the vanadate anion inhibits ATP hydrolysis by entering into reaction with the Ca^{2+}-ATPase either as an inorganic orthophosphate or as a transition state analogue.

The maximum number of binding sites for decavanadate is about 150 nmol V/mg protein, i.e. about 10–18 times greater than that of monovanadate. Therefore at saturation about 1.4–2.1 mol decavanadate ($V_{10}O_{28}^{6-}$) is bound/mol Ca^{2+}-ATPase; the apparent affinity constant is about 10 times greater than that of the monovanadate binding, when expressed in decavanadate units.

These observations raise the possibility that monovanadate and decavanadate may occupy the same binding site

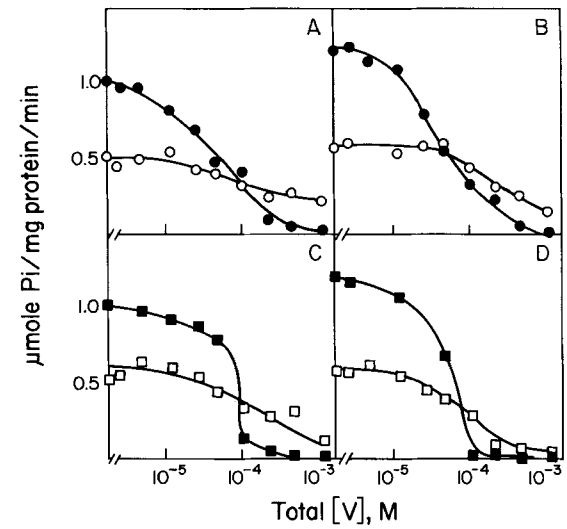

Fig. 7. *The effect of monovanadate and decavanadate on the ATPase activity of microsomes.* Sarcoplasmic reticulum vesicles were preincubated at 2°C in 0.1 M KCl, 10 mM imidazole pH 7.4, 5 mM $MgCl_2$, and 0.5 mM EGTA for 24 h (A and C) or for 2 h (B and D). This was followed by incubation with monovanadate (○, ●) for 2 h (A) or 24 h (B), or with decavanadate (□, ■) for 2 h (C) or 24 h (D), at the concentrations indicated on the abscissa. All concentrations are expressed as molar monovanadate. Open symbols: samples without A23187. Filled symbols: samples with 2 μM A23187. At the end of preincubation, samples were taken for the assay of ATPase activity as described under Methods. The Ca^{2+}-modulated component of ATP hydrolysis was calculated by correcting the total ATPase activity for the basal Ca^{2+}-insensitive ATP hydrolysis

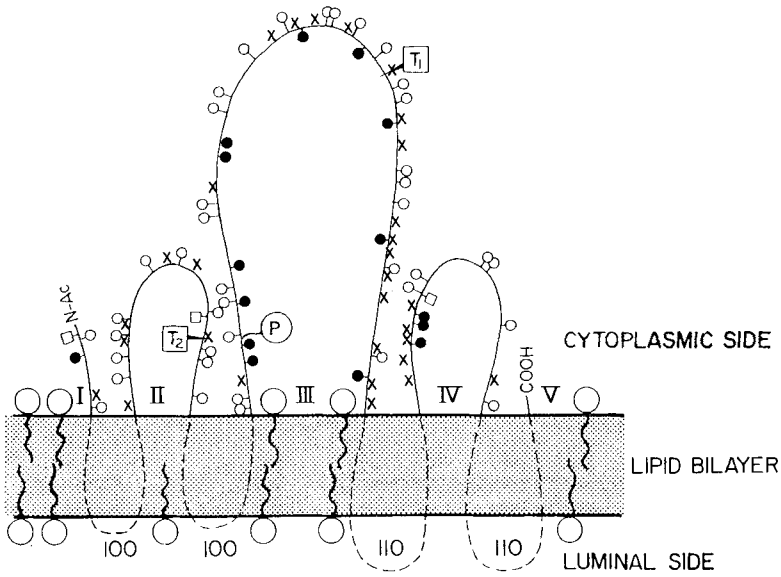

Fig. 8. *The hypothetical structure of the Ca^{2+}-ATPase of sarcoplasmic reticulum.* The five established amino acid sequences correspond to regions I – V exposed on the cytoplasmic surface of the sarcoplasmic reticulum membrane. The phospholipid bilayer is indicated as the shaded layer through which the unsequenced transmembrane segments of the Ca^{2+}-transport ATPase are assumed to penetrate. It is presumed that each of these hydrophobic segments contain about 100 – 110 amino acid residues permitting several transmembrane folds in the ATPase structure. The phosphate-acceptor aspartyl residue is denoted as P; the primary tryptic cleavage site that yields the A and B fragments is at T_1. The secondary tryptic cleavage site that yields the A_1 and A_2 fragments is at T_2. Both T_1 and T_2 are adjacent to arginine residues. (□) Histidine; (○) lysine; (●) cysteine; (×) arginine. The NH_2 terminal is in sequence I, the COOH terminal is in sequence V. The presumed location of the vanadate-binding site is in the region between T_2 and P. (Adapted from [35])

on the Ca^{2+}-ATPase, and the occupancy of these sites by either monovanadate or decavanadate inhibits the ATPase activity. Should this be the case, the inhibition of ATPase activity by decavanadate may also involve the trapping of the enzyme in the E_2-V form. Although additional binding of decavanadate at secondary site(s) may occur at higher concentrations, further investigation is needed to establish this possibility.

The binding of both $H_2VO_4^-$ and $V_{10}O_{28}^{6-}$ at the phosphate/ATP binding site of the Ca^{2+}-ATPase suggests that the structure of the vanadate binding site is sufficiently open or flexible to accomodate either of the two vanadate species despite their rather different size and shape. The greater affinity of $V_{10}O_{28}^{6-}$ as compared with $H_2VO_4^-$ for the binding site is best explained if electrostatic forces play an important role in the interaction, which in turn suggests that the binding site is rich in positively charged groups such as lysine and arginine.

The studies of Allen, Green and their colleagues [31 – 34] defined the amino acid sequence of five major hydrophilic segments of the Ca^{2+}-transport ATPase that are presumed to be exposed on the cytoplasmic surface of the membrane. These segments are probably connected by four relatively hydrophobic intramembranous stretches of polypeptide chains, each consisting of about 100 amino acids, that anchor the Ca^{2+}-transport ATPase to the phospholipid bilayer (Fig. 8) [35].

The phosphate-acceptor aspartyl residue is located in sequence 3 surrounded by a relatively high density of lysine and arginine residues. A lysine residue near the phosphorylation site was tentatively identified as 'essential' for activity, since its reaction with pyridoxal 5 -phosphate caused inactivation of the Ca^{2+}-transport ATPase which could be prevented by either Ca^{2+} or by ATP [34 – 36]. The Ca^{2+}-transport activity is also inhibited by reaction of lysine residues with fluorescein isothiocyanate [37, 38] or with fluorescamine [39] and these effects are also blocked by ATP. Thus the region of the ATPase molecule that serves as phosphate acceptor and binds the substrates and substrate analogs (phosphate, ATP and vanadate) is likely to contain several functionally important basic amino acids. From the effects of pH, Ca^{2+}, vanadate and P_i upon the fluorescence of fluorescein isothiocyanate covalently bound to the Ca^{2+}-ATPase, Pick and Karlish [11] suggested that the affinity of the E_1 form for Ca^{2+} is high and for H^+ is low, while in the E_2 form the reverse is true. These differences in the acid-base character of the active site may contribute to the selective binding of V to the E_2 conformation of the enzyme.

Tryptic cleavage of the Ca^{2+}-transport ATPase into two major fragments (A and B) at the T_1 site (Fig. 8) did not interfere with the vanadate-induced formation of Ca^{2+}-ATPase membrane crystals [2]. The ability of Ca^{2+}-transport ATPase to crystallize was lost after further cleavage of the A fragment into A_1 and A_2 subfragments at the T_2 site; this cleavage is known to be accompanied by loss of Ca^{2+} uptake [2]. Vanadate (0.1 – 5 mM) inhibited the secondary cleavage of Ca^{2+}-ATPase by trypsin at the T_2 site [2]. The vanadate-induced change in the susceptibility of the T_2 site may result from direct blocking of the site by vanadate or from a change in the conformation of the enzyme by vanadate bound elsewhere in the molecule. We propose, based on the amino acid sequence of Ca^{2+}-ATPase shown in Fig. 8, that in the native structure the T_2 site is in the vicinity of the phosphate-acceptor aspartyl residue and may be part of the binding site for phosphate, ATP and vanadate. In such a case the influence of vanadate [2] and ATP [40, 41] on the sensitivity of the T_2 site for tryptic cleavage may be a direct influence of the ligands bound near the T_2 site. The T_2 region of the Ca^{2+}-ATPase is also relatively rich in lysine [34]. Together with the arginine at the T_2 site, these basic residues may contribute to the high

positive-charge density of the vanadate binding site. If tryptic cleavage at the T_2 site or treatment of microsomes with pyridoxal phosphate, fluorescamine or fluorescein isothiocyanate would inhibit both vanadate binding and the vanadate-induced crystallization of the Ca^{2+}-ATPase, this suggestion would be considerably strengthened.

The rate of crystallization of the Ca^{2+}-ATPase is dramatically accelerated by increasing the vanadate concentration to 5 mM, where nearly complete crystallization can be achieved in less than 4 h [2]. In a 5 mM vanadate solution at pH 7.4, vanadate oligomers (dimers, tetramers, etc.) are the dominant species. Decavanadate solutions induce 50% crystallization within 4 h at a total V concentration of only 0.25 mM. These observations clearly indicate that vanadate polymers, especially decavanadate, are effective inducers of the crystallization of Ca^{2+}-ATPase. This effectiveness may arise in part from the high affinity of decavanadate for the binding sites of the Ca^{2+}-ATPase and from the fact that at saturating concentrations, the number of moles of V bound per mole of Ca^{2+}-ATPase is about 10 times greater with decavanadate than with monovanadate. The occupation of the vanadate binding site by the octahedral $V_{10}O_{28}^{6-}$ may impose a coordination geometry somewhat different from that obtained with monomeric vanadium (V) or with the tetrahedral vanadate dimers, tetramers and hexamers. Furthermore, the charge distribution of the active site is expected to be different with bound $V_{10}O_{28}^{6-}$, than in the presence of $H_2VO_4^-$. Since the ATPase-ATPase interactions required for the formation of ATPase crystals are influenced by surface charges [3, 4], the effectiveness of decavanadate in promoting the crystallization of Ca^{2+}-ATPase may result from effective neutralization of charge repulsions. These observations imply that, in addition to the previously proposed trapping of the Ca^{2+}-ATPase in the E_2-V form, by acting as a phosphate analogue, vanadate may affect the conformation of the Ca^{2+}-ATPase through coordination and charge effects. Through such effects, vanadate may create conformational states that are highly favorable for crystallization, but differ from the 'physiological' conformational states that occur during ATP-dependent Ca^{2+} transport. The magnitude of such differences could be assessed only by comparing the three-dimensional structures of the Ca^{2+}-ATPase reconstructed from crystals obtained with inorganic phosphate, monovanadate, and decavanadate, as inducers of the putative E_2 conformation. Similar caution is required in the identification of the Ca^{2+}-ATPase crystal structures obtained with Gd^{3+} or La^{3+} [42, 43] as being representative of the E_1 conformation.

We thank Dr Kenneth Kustin (Department of Chemistry, Brandeis University, Waltham, Massachusetts) for his interest and suggestions that significantly aided our work. This work was supported by research grants from the National Institutes of Health (AM 26545), the National Science Foundation (PCM 84-03679) and the Muscular Dystrophy Association.

REFERENCES

1. Dux, L. & Martonosi, A. (1983) *J. Biol. Chem. 258*, 2599–2603.
2. Dux, L. & Martonosi, A. (1983) *J. Biol. Chem. 258*, 10111–10115.
3. Dux, L. & Martonosi, A. (1983) *J. Biol. Chem. 258*, 11896–11902.
4. Dux, L. & Martonosi, A. (1983) *J. Biol. Chem. 258*, 11903–11907.
5. Dux, L. & Martonosi, A. (1983) *Muscle & Nerve 6*, 566–573.
6. Taylor, K. A., Dux, L. & Martonosi, A. (1984) *J. Mol. Biol. 174*, 193–204.
7. Beeler, T. J., Dux, L. & Martonosi, A. (1984) *J. Membr. Biol. 78*, 73–79.
8. Peracchia, C., Dux, L. & Martonosi, A. (1984) *J. Muscle Res. Cell Motil. 5*, 431–442.
9. Dux, L. & Martonosi, A. (1984) *Eur. J. Biochem. 141*, 43–49.
10. Pick, U. (1982) *J. Biol. Chem. 257*, 6111–6119.
11. Pick, U. & Karlish, S. D. (1982) *J. Biol. Chem. 257*, 6120–6126.
12. Boyd, D. W. & Kustin, K. (1984) *Adv. Inorg. Biochem. 6*, 311–365.
13. Baes, C. F. & Mesmer, R. E. (1976) *The hydrolysis of cations*, Wiley, New York.
14. Chasteen, N. D. (1983) *Struct. Bonding 53*, 105–138.
15. Choate, G. & Mansour, T. E. (1979) *J. Biol. Chem. 254*, 11457–11462.
16. DeMaster, E. G. & Mitchell, R. A. (1973) *Biochemistry 12*, 3616–3621.
17. Sachsenheimer, W. & Schulz, G. E. (1977) *J. Mol. Biol. 114*, 23–36.
18. Pai, E. F., Sachsenheimer, W., Schirmer, R. H. & Schulz, G. E. (1977) *J. Mol. Biol. 114*, 37–45.
19. Climent, F., Bartrons, R., Pons, G. & Carreras, J. (1981) *Biochem. Biophys. Res. Commun. 101*, 570–576.
20. Soman, G., Chang, Y. C. & Graves, D. J. (1983) *Biochemistry 22*, 4994–5000.
21. Kustin, K. & Macara, I. G. (1982) *Commun. Inorg. Chem. 2*, 1–22.
22. Nakamura, H., Jilka, R. L., Boland, R. & Martonosi, A. (1976) *J. Biol. Chem. 251*, 5414–5423.
23. Luftig, R. B. (1968) *J. Ultrastruct. Res. 23*, 178–181.
24. Goodno, C. C. (1979) *Proc. Natl Acad. Sci. USA 76*, 2620–2624.
25. Medda, P. & Hasselbach, W. (1983) *Eur. J. Biochem. 137*, 7–14.
26. Lowry, O. H., Rosebrough, N. J. & Farr, A. L. & Randall, R. J. (1951) *J. Biol. Chem. 193*, 265–275.
27. Fiske, C. H. & Subbarow, Y. (1925) *J. Biol. Chem. 66*, 375–400.
28. Goddard, J. B. & Gonas, A. M. (1973) *Inorg. Chem. 12*, 574–579.
29. Druskovich, D. M. & Kepert, D. L. (1976) *J. Chem. Soc. Dalton Transact.* 947–951.
30. Duggan, P. F. & Martonosi, A. (1970) *J. Gen. Physiol. 56*, 147–167.
31. Allen, G. (1980) *Biochem. J. 187*, 545–563.
32. Allen, G. (1980) *Biochem. J. 187*, 565–575.
33. Allen, G., Bottomley, R. C. & Trinnaman, B. J. (1980) *Biochem. J. 187*, 577–589.
34. Allen, G., Trinnaman, B. J. & Green, N. M. (1980) *Biochem. J. 187*, 591–616.
35. Ikemoto, N. (1982) *Annu. Rev. Physiol. 44*, 297–317.
36. Murphy, A. J. (1977) *Arch. Biochem. Biophys. 180*, 114–120.
37. Pick, U. & Karlish, S. J. D. (1980) *Biochim. Biophys. Acta 626*, 255–261.
38. Pick, U. & Bassilian, S. (1981) *FEBS Lett. 123*, 127–131.
39. Hidalgo, C., Petrucci, D. A. & Vergara, C. (1982) *J. Biol. Chem. 257*, 208–216.
40. Saito, K., Imamura, Y. & Kawakita, M. (1984) *J. Biochem. (Tokyo) 95*, 1297–1304.
41. Imamura, Y., Saito, K. & Kawakita, M. (1984) *J. Biochem. (Tokyo) 95*, 1305–1313.
42. Dux, L., Taylor, K. A. & Martonosi, A. (1984) *Fed. Proc. 43*, 1700.
43. Martonosi, A., Kracke, G., Taylor, K. A., Dux, L. & Peracchia, C. (1985) in *Regulation and development of membrane transport processes* (Graves, J., ed.) pp. 57–85, Wiley, New York.